

Final Technical Report for:  
**ErAs/GaAs SUPERLATTICE INFRARED DETECTOR**  
**BY CHEMICAL VAPOR DEPOSITION**

Submitted under  
 Contract No. F49620-93-C-0033

Covering the period:  
 1 July 1993 - 31 December 1993

Accesion For	
NTIS	CRA&I
DTIC	TAB
Unannounced	<input checked="" type="checkbox"/>
Justification	
By _____	
Distribution / _____	
Availability Codes	
Dist	Avail and/or Special
A-1	

Submitted to:  
 Air Force Office of Scientific Research  
 110 Duncan Avenue, Suite B115  
 Bolling AFB, DC 20331-0001

Submitted by:  
 Spire Corporation  
 One Patriots Park  
 Bedford, MA 01730-2396

19950323 120

FR-60290

WOSRTR 95 0146

A Final Technical Report for  
**E-As/GaAs SUPERLATTICE  
INFRARED DETECTOR BY  
CHEMICAL VAPOR  
DEPOSITION**

Submitted under:  
**Contract No. F49620-93-C-0033**

Submitted to:  
**Air Force Office of Scientific Research/PKA  
110 Duncan Avenue, Suite B115  
Bolling AFB, DC 20332-0001**

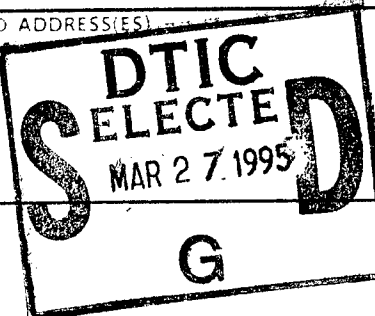


**spire**

# REPORT DOCUMENTATION PAGE

Form Approved  
OMB No. 0704-0188

Public reporting burden for this collection of information is estimated to average 1 hour per response, including the time for reviewing instructions, searching existing data sources, gathering and maintaining the data needed, and completing and reviewing the collection of information. Send comments regarding this burden estimate or any other aspect of this collection of information, including suggestions for reducing this burden, to Washington Headquarters Services, Directorate for Information Operations and Reports, 1215 Jefferson Davis Highway, Suite 1204, Arlington, VA 22202-4302, and to the Office of Management and Budget, Paperwork Reduction Project (0704-0188), Washington, DC 20503.

1. AGENCY USE ONLY (Leave blank)	2. REPORT DATE	3. REPORT TYPE AND DATES COVERED <b>FINAL</b>	
4. TITLE AND SUBTITLE <b>ErAs/GaAs Superlattice Infrared Detector by Chemical Vapor Deposition</b>			5. FUNDING NUMBERS <b>61102F 3005/SS</b>
6. AUTHOR(S) <b>Dr Greenwald</b>			
7. PERFORMING ORGANIZATION NAME(S) AND ADDRESS(ES) <b>Spire Corporation</b>			8. PERFORMING ORGANIZATION REPORT NUMBER <b>AFOSR-TR- 95 0140</b>
9. SPONSORING MONITORING AGENCY NAME(S) AND ADDRESS(ES) <b>AFOSR/NE 110 Duncan Avenue Suite B115 Bolling AFB DC 20332-0001</b>			10. SPONSORING MONITORING AGENCY REPORT NUMBER <b>F49620-93-C-0033</b>
11. SUPPLEMENTARY NOTES			
			
12a DISTRIBUTION AVAILABILITY STATEMENT <b>APPROVED FOR PUBLIC RELEASE: DISTRIBUTION UNLIMITED</b>		12b DISTRIBUTION CODE	
13. ABSTRACT (MAXIMUM 250 WORDS)			
<b>SEE FINAL REPORT ABSTRACT</b>			
14. SUBJECT TERMS			15. NUMBER OF PAGES
17. SECURITY CLASSIFICATION OF REPORT <b>UNCLASSIFIED</b>	18. SECURITY CLASSIFICATION OF THIS PAGE <b>UNCLASSIFIED</b>	19. SECURITY CLASSIFICATION OF ABSTRACT <b>UNCLASSIFIED</b>	20. LIMITATION OF ABSTRACT <b>UNCLASSIFIED</b>

## TABLE OF CONTENTS

	<u>Page</u>
PREFACE .....	vi
1 SUMMARY .....	1
2 INTRODUCTION .....	2
2.1 Related Research by Other Workers .....	3
3 EXPERIMENTAL PROCEDURES .....	5
4 RESULTS .....	7
5 CONCLUSIONS AND RECOMMENDATIONS .....	14
6 REFERENCES .....	15
LIST OF SYMBOLS, ABBREVIATIONS, and ACRONYMS .....	16

## LIST OF FIGURES

	<u>Page</u>
1 ErAs/GaAs Superlattice photovoltaic infrared detector .....	3
2 Schematic diagram of hot wall reactor .....	6
3 Auger spectroscopy data of erbium film deposited in the presence of hydrogen on GaAs without arsine or TBA .....	7
4 Auger spectroscopy data for an ErAs film deposited from Er(Cp) <sub>3</sub> with TBA in the presence of hydrogen with slight oxygen leak .....	8
5 RBS data of sample 1879 showing deposition of thin ErAs layer epitaxial relationship through small $\chi_{\min}$ .....	10
6 SIMS data of sample 1879 showing diffusion tails of erbium moving into bulk GaAs, also deep low concentration erbium film not visible with RBS .....	11
7 SIMS data of sample 1876 with largest erbium concentration, one atomic percent .....	11
8 X-ray rocking curve for <200> reflection from sample 1878 showing good crystal quality .....	12
9 High magnification TEM microphotograph of erbium doped GaAs layer showing one defect at start of growth (arrow), and terraced surface from substrate alignment 1° off true <100> .....	13

## LIST OF TABLES

	<u>Page</u>
1 Deposition conditions .....	5
2 Experimental matrix for ErAs deposition from Er(MeCp) <sub>3</sub> plus arsine .....	9
3 Time-temperature profiles for two deposition runs .....	9

## PREFACE

This scientific study was supported by the Air Force Office of Scientific Research out of Bolling Air Force Base, Washington DC.

We would also like to recognize the help of Prof. William Rees, Jr. of Georgia Technical Institute who first synthesized the erbium amide compound used in this study.

## **1 SUMMARY**

The overall goal of this research program was to determine if a superlattice structure of a III-V semiconductor compound (GaAs) and a IIIA-V semi-metal compound (ErAs) would form a low bandgap semiconductor material which could be used as a longwave infrared detector. For reference, a superlattice of the semi-metal HgTe and the semiconductor CdTe will work as an infrared detector. Production of the combination, however, is not practical and the compound  $Hg_xCd_{1-x}Te$  is more widely utilized.

The technical objective of this SBIR Phase I program was to demonstrate heteroepitaxial growth of the semi-metallic compound erbium-arsenide on top of a single crystal GaAs substrate, and then demonstrate heteroepitaxial growth of GaAs on top of this structure. This would demonstrate feasibility of fabricating the superlattice structure.

Spire successfully demonstrated epitaxial growth of a GaAs/(Er,Ga)As/GaAs structure using metalorganic chemical vapor deposition (MOCVD) with tris(trimethyl-disilyl-amido) erbium and arsine. Rapid diffusion of erbium during growth of the top GaAs layer at 650°C precluded a pure ErAs layer being realized in the sandwiched structure. While reduced growth temperature might allow realization of a superlattice structure, a lower risk alternate application of heteroepitaxial erbium-arsenide/gallium-arsenide was proposed for Phase II development.

For this research, Spire tested three different sources of erbium including the cyclopentadienyl, methyl-cyclopentadienyl, and amide derivatives and two arsenic sources including arsine and tertiarybutyl arsine. The composition of films was measured by Auger, SIMS, and RBS analyses. RBS and TEM results indicated the structure of films grown for this program. All combinations of the source materials except that of arsine and the erbium amide left excess carbon in the deposited film.

## 2 INTRODUCTION

There are presently no satisfactory silicon or GaAs-compatible sensors for detection of infrared radiation at wavelengths longer than 5  $\mu\text{m}$ . Compatibility with standard semiconductor technology is crucial for focal plane array applications where a high density of devices with uniform properties is required. Uniform solid solutions of (Hg,Cd)Te, while theoretically capable of meeting these requirements, have proven very difficult to fabricate.

Superlattices of HgTe/CdTe have been proposed for detectors.<sup>1</sup> By tailoring the layer thickness in the superlattices, the effective bandgap of the material may be varied from that of the semi-metallic HgTe (0 eV) to that of the semiconducting CdTe (1.6 eV). Thus, the cutoff wavelength for detection of radiation may be adjusted by varying layer thickness. The quantum efficiency for this process is sufficient for use of these structures for long wavelength infrared sensing. In the ten years since this paper was published, there has not been sufficient advance in processing technology to commercially produce Hg, Cd, and Te structures. Also, it is extremely difficult to grow such materials epitaxially on silicon or GaAs. Semiconductor compatibility is extremely desirable for monolithic integration of the sensor and controlling electronics.

An alternate material, LaN, has been suggested.<sup>2</sup> LaN is a semi-metal with a crystal structure suggesting it can be grown epitaxially on silicon. A superlattice of LaN and Si would have an effective bandgap that could be adjusted from that of LaN (0 eV) to that of silicon (1.1 eV). Such a superlattice would detect infrared radiation through photoexcitation of carriers across this gap, a high quantum efficiency process. To date, there have been no experimental results published on LaN:Si superlattices.

The objective of this research was to test the equivalent to LaN:Si and HgTe:CdTe superlattices in III-V compound semiconductors using the near lattice-matched semi-metallic alloy ErAs (5.74 $\text{\AA}$ ) with GaAs (5.65 $\text{\AA}$ ). If good quality superlattices of ErAs and GaAs can be grown, one would expect to be able to obtain effective bandgaps ranging from 0 eV (since LaN is semi-metallic) to 1.4 eV, the bandgap of GaAs. There is a practical limit to very small bandgaps imposed by the variations in layer thickness. However, gaps down to 0.1 eV are feasible. This would allow detection of radiation out to at least 12  $\mu\text{m}$ , covering the range of greatest interest, the atmospheric window at 8 to 14  $\mu\text{m}$ .

The novel feature of this concept is heteroepitaxial growth of an ErAs/GaAs superlattice by metalorganic chemical vapor deposition (MOCVD). MOCVD of erbium compounds has only recently been made possible with the development of suitable sources for this element.<sup>3</sup> MOCVD of ErAs has not previously been reported. Deposition of this compound on GaAs is considered the key technical difficulty, fewer problems are expected with deposition of GaAs on ErAs, aside from possible interdiffusion of erbium and gallium.

One possible design of a photodetector based upon ErAs-GaAs superlattices is shown in Figure 1, after reference [2], which suggests the use of MBE for the fabrication technique. Good quality superlattices of III-V semiconductors are grown in production quantities by MOCVD at Spire at lower costs than can be achieved by MBE, and in this case the vapor process may prove superior.

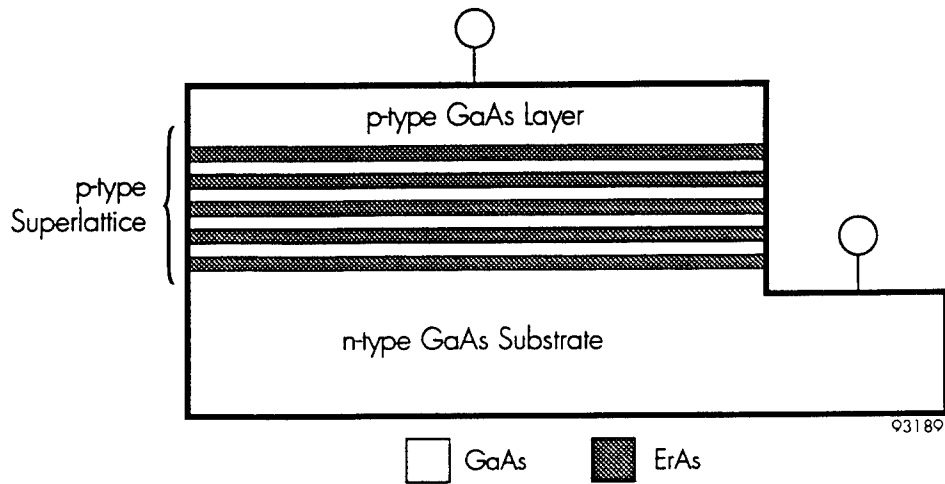


**Figure 1** *ErAs/GaAs superlattice photovoltaic infrared detector.*

The objective of this Phase I SBIR research was to show the feasibility of the novel concept for the final product; heteroepitaxy of ErAs on GaAs by chemical vapor deposition (CVD). A second, subsequent objective was to show heteroepitaxy of GaAs on ErAs. Intermediate objectives were:

- (1) Demonstrate deposition of ErAs at temperatures and pressures consistent with deposition of high quality GaAs films.
- (2) Demonstrate epitaxial deposition of smooth and continuous ErAs films on GaAs.
- (3) Demonstrate deposition of epitaxial and continuous GaAs films on ErAs.

## 2.1 Related Research by Other Workers

Epitaxial growth of ErAs on GaAs and of GaAs on ErAs by MBE has been studied by Bellcore for many years for potential use as ohmic contact technique to GaAs structures.<sup>4-9</sup> Similar work has also been reported by workers in Germany,<sup>10</sup> and in France.<sup>11</sup> In all cases, thin layers have been grown with minimal defects. The difference in structure, zinc-blend for GaAs versus NaCl for ErAs, introduces some defects twinning in multilayer structures. Improved results were noted for growth of GaAs on top of  $\text{Er}_x\text{Sc}_{1-x}\text{As}$  films grown on <111> GaAs.

MOCVD of Er in GaAs as a dopant had been previously reported.<sup>12,13,14</sup> There were no data on MOCVD of ErAs. The work referred to does not indicate whether results from MOCVD of ErAs on GaAs would be better or worse than MBE results.

One recent study of ErAs layers as thin as 3 Å sandwiched between GaAs material implied that ErAs will always behave as a semi-metal, and that a superlattice of ErAs/GaAs will never behave as a low bandgap semiconductor.<sup>15</sup> There were defects in the upper layer of GaAs deposited on top of the ErAs layer and this may change results for materials with fewer defects. Exact lattice-matching with the addition of phosphorus to the GaAs compounds and/or the addition of scandium to the erbium compound may also change properties.

### 3 EXPERIMENTAL PROCEDURES

We used metalorganic chemical vapor deposition (MOCVD) to deposit both ErAs and the top layer of GaAs-on-GaAs substrates. A cold wall, induction heated reactor was utilized (Table 1). Initial experimental design called for all tests to be conducted with tertiarybutyl arsine, a liquid precursor that is safer to handle than arsine gas. However, when this chemistry left an excess of carbon in all deposited films, work was shifted to another available facility that was modified to add erbium sources.

**Table 1** *Deposition conditions.*

Heating Method	Induction
Pressure	75 torr
Temperature (°C)	500, 650
Total Flow Rate	2 & 5 slpm
Carrier gas/diluent	hydrogen
arsenic precursor	arsine tertiarybutylarsine
erbium precursors	methylcyclopentadienyl Er erbium amide

A schematic diagram of the deposition facility is shown in Figure 2. The reactor is a quartz bell jar with a coated graphite susceptor. A water cooled copper coil wrapped around the outside carried tuned RF current which heats the SiC coated susceptor. The susceptor turned at about 2 rpm for improved uniformity.

The gas delivery system is all welded and inside gas cabinets for safety. Hydrogen was used for a carrier gas as well as a diluent. Total flow into the reactor was either 2 or 5 slpm. Flow rates were measured by electronic mass flow controllers accurate to 0.5%. Liquid sources for gallium (trimethyl gallium) and arsenic (tertiarybutyl arsine) were cooled below room temperature to 6 and 20°C respectively. Temperatures were controlled to  $\pm 0.01^\circ\text{C}$ . The pressure in these two sources was also controlled to  $\pm 1\%$  using capacitance manometers and variable control valves; typical setting was 700 torr. The rate of delivery of these source compounds was reproducible with an accuracy of about 2%.

Metalorganic erbium compounds have negligible vapor pressure until heated above 150°C. As this temperature is beyond tolerable limits for either available variable valves or accurate pressure sensors, the erbium sources were used without pressure controls. The pressure believed to exist in the bubblers is close to that of the reactor, about 75 torr. The rate of carrier gas flow (between 50 and 200 sccm) was measured as for other sources. Temperature of the erbium source (200 for Cp, 180 for MeCp, and 170 for the amide) was regulated through the use of an oil bath with nominal control of  $\pm 0.03^\circ\text{C}$ .

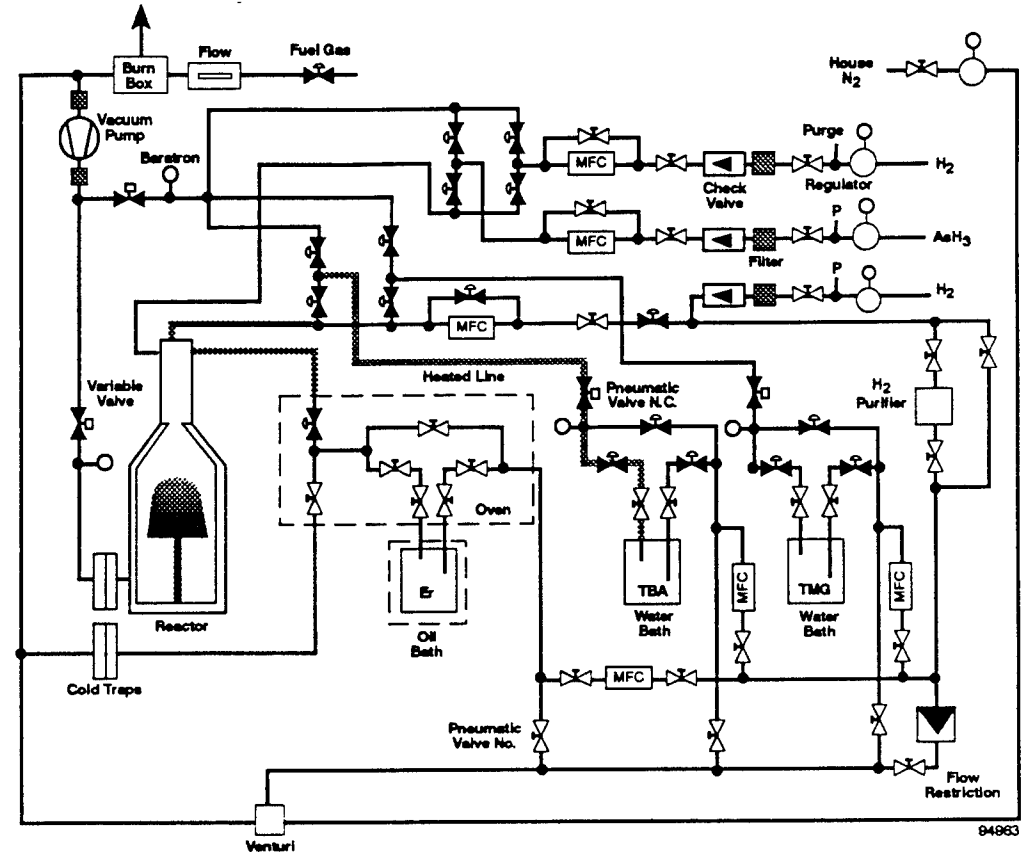


**Figure 2      Schematic diagram of hot wall reactor.**

For safety considerations, the vacuum pump was configured for handling toxic gases and filled with fomblin oil to allow high concentrations of oxygen. There were particulate filters before the pump and mist filters after the pump as well as a separate filter for the pump oil to remove particulates and neutralize acid build up. Exhaust from the pump was run through a burn-off to assure combustion of all products and unreacted source material. Burnoff products were  $\text{CO}_2$ ,  $\text{H}_2\text{O}$ , and fine solid oxide particulate. This particulate was removed from effluent discharged into the atmosphere by HEPA filters.

Substrates used for deposition of erbium arsenide were semi-insulating GaAs <100> orientation, silicon <111> orientation, silicon with a thermal oxide ( $\text{SiO}_2$ ) coating, and some platinum coated silicon wafers with an oxide diffusion barrier layer between the metal and substrate. Films on the GaAs substrates were analyzed most extensively, other materials were chosen to aid identification of erbium deposition and proper source operation.

## 4 RESULTS

Spire demonstrated epitaxial growth of (Er,Ga)As with erbium concentrations up to ten atomic percent. Pure erbium arsenide was not detected due to interdiffusion of erbium and gallium metal atoms.

Without the presence of tertiarybutyl arsine (TBA) or arsine, the cyclopentadienyl erbium compounds decomposed on the GaAs surface to synthesize erbium carbide. This is shown in the Auger spectroscopy data on Figure 3. Oxidation of this film was originally believed to result from atmospheric exposure after deposition.

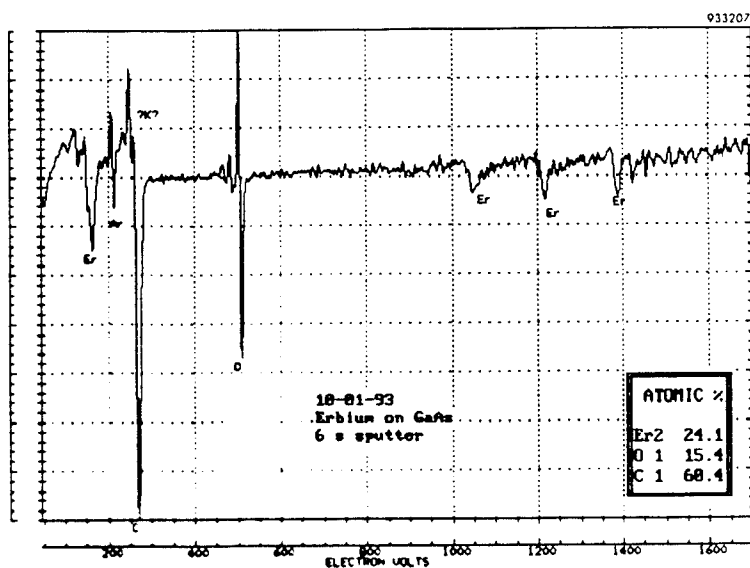


**Figure 3** Auger spectroscopy data of erbium film deposited in the presence of hydrogen on GaAs without arsine or TBA.

When the same source, Er (Cp), was used for deposition of films in the presence of TBA, the carbon content of the film was reduced, as shown in Figure 4. The high oxygen content of the films in Figures 3 and 4 was, after the fact, traced to a leak in the reactor vessel and gas transport system. To reduce the oxygen levels, the experiment was shifted to a similar but newer reactor. Note that there is no significant amount of gallium near the surface of these films.

In the new reactor, the arsenic source was changed to arsine gas and the erbium sources tested were now Er(MeCp), and the erbium amide. For the methylcyclopenta-dienyl compound, a matrix of deposition runs was attempted but the erbium source was depleted during the experiment, after run 1879. For all deposition runs listed in Table 2, the sequence of film growth was identical (Table 3). First the reactor and erbium transport lines were purged and the sources were heated. Second, the sample was heated in an overpressure of arsine (to prevent decomposition of the GaAs surface). Third, a 300 nm GaAs buffer layer was grown at 650°C and the reactor was purged of gallium afterwards. Fourth, the erbium source was turned from vent to growth and the reactor cooled (if necessary). Growth time was 15 to 30 minutes at the temperature indicated in Table 2. Fifth, a cap layer of ~60 nm of GaAs was deposited at 650°C prior to cool down and final purging.

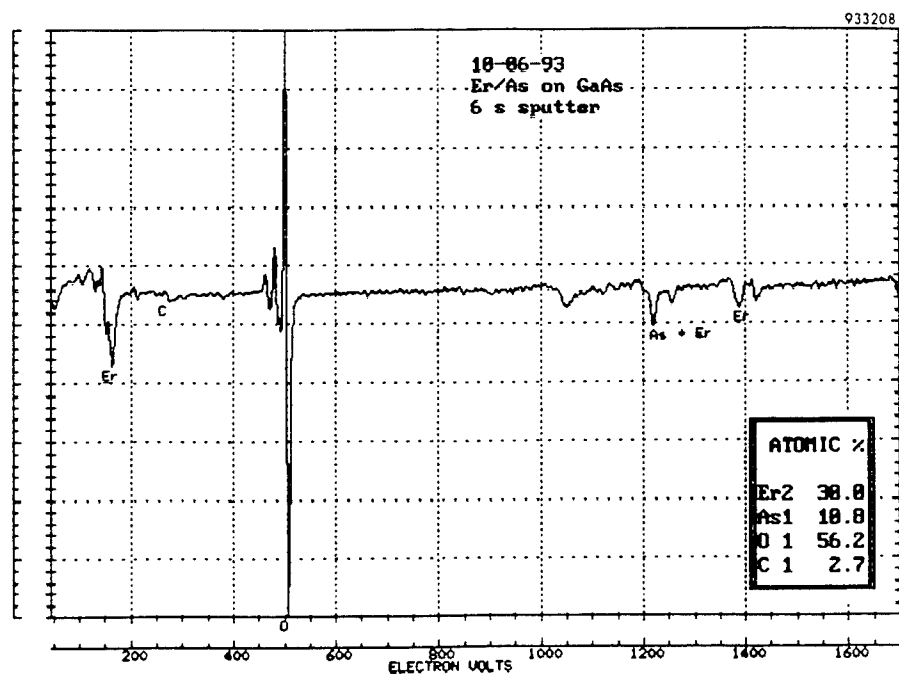


**Figure 4** Auger spectroscopy data for an ErAs film deposited from  $\text{Er}(\text{Cp})_3$  with TBA in the presence of hydrogen with slight oxygen leak.

**Table 2** Experimental matrix for ErAs deposition from  $\text{Er}(\text{MeCp})_3$  plus arsine.

MOCVD Run #	Temp. (°C)	Press. (torr)	Total Flow (sccm)	Carrier Flow (sccm)	Arsine Flow (sccm)
1876	650	50	2	1600	50
1877	650	50	2	800	50
1878	650	200	5	50	50
1879	500	200	5	800	50
1880	500	50	2	50	50
1881	650	200	2	50	335
1882	650	50	5	800	335
1883	500	200	2	800	335
1884	500	50	5	50	335

**Table 3** Time-temperature profiles for two deposition runs.

1876		1879		Description of Deposition Step
Temp. (°C)	Time (sec)	Temp. (°C)	Time (sec)	
100	10	100	10	purge and start arsine flow
650	600	650	600	heat up substrate, Er bypass flowing to reactor
650	15	650	15	increase arsine flow
650	300	650	300	deposit GaAs buffer layer
650	30	500	600	cool down and/or purge Ga flow
650	1800	500	900	erbium arsenide deposition
650	30	650	600	heat up and/or purge Er flow
650	60	650	60	deposit capping GaAs layer
100	900	100	900	cool down
100	10	100	10	turn off arsine flow and purge

When the experiment was complete and the source was changed, technicians discovered that some of the source material had been pushed into the gas inlet lines of the bubbler, and into the bypass line around the source. As this bypass line was purged through the reactor before deposition was to begin, some small amount of erbium was deposited on top of the substrate prior to deposition of the GaAs buffer. This accounts for the very deep, but low level erbium peak in the SIMS analyses of these samples.

The results of these experiments are summarized in Figure 5, Rutherford backscattering spectroscopy (RBS) data, and in Figures 6 and 7, secondary ion mass spectroscopy (SIMS) data. Figure 5 shows that the high concentration erbium arsenide layer was very narrow, 40 nm, with a peak concentration of 0.25 atomic percent, or approximately  $1.1 \times 10^{20} \text{ cm}^{-3}$ . A comparison of the random and channeling spectra shown in Figure 5, a ratio called  $\chi_{\min}$ , indicates that only 12% of the erbium was substitutional in the GaAs lattice. The substitutional fraction of erbium, about  $10^{19} \text{ cm}^{-3}$ , could be interpreted as the solid solubility limit for erbium in GaAs grown by MOCVD at 650°C. The GaAs capping layer was epitaxial (with low  $\chi_{\min}$  of 5.1%) to the erbium containing layer and to the substrate. One question remains, "why was the peak concentration of erbium only 0.25 atomic percent?"

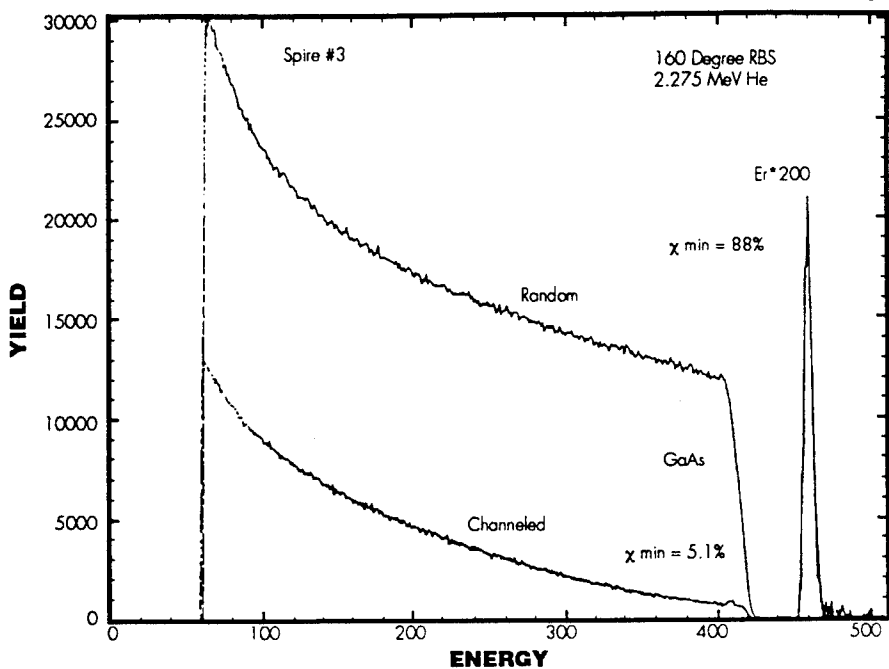


**Figure 5** RBS data of sample 1879 showing deposition of thin ErAs layer epitaxial relationship through small  $\chi_{\min}$ .

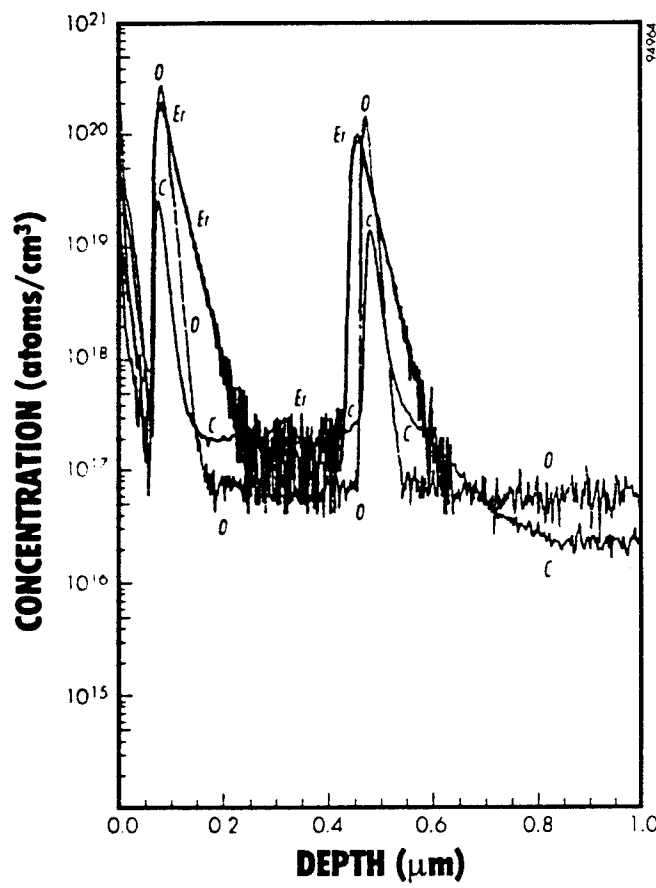


**Figure 6** SIMS data of sample 1879 showing diffusion tails of erbium moving into bulk GaAs, also deep low concentration erbium film not visible with RBS.

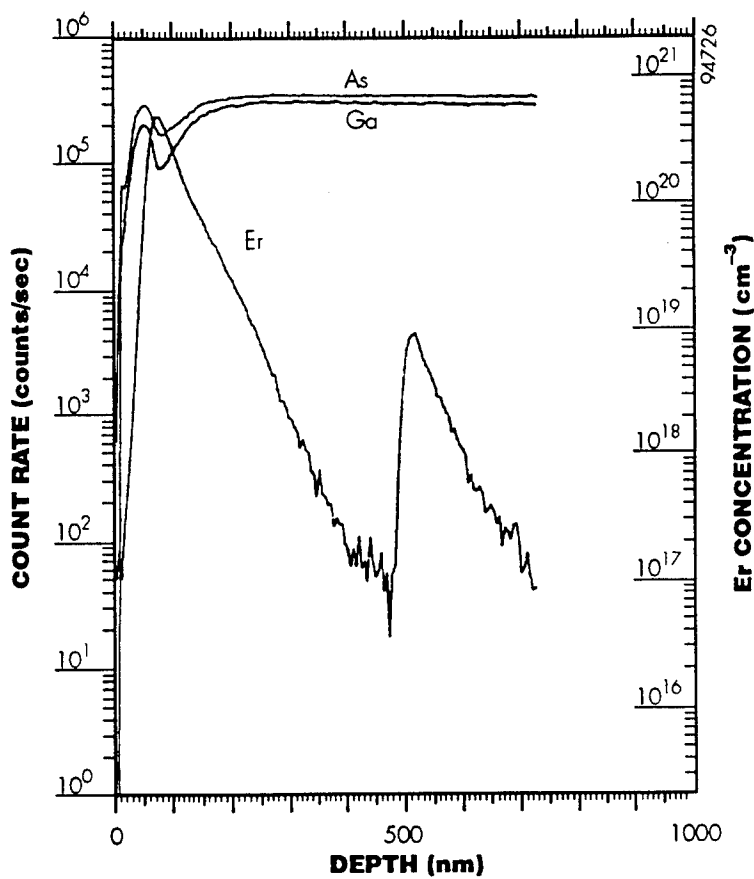


**Figure 7** SIMS data of sample 1876 with largest erbium concentration, one atomic percent.

Data in Figure 6, for the same sample as in Figure 5, indicate that erbium diffusion may be responsible for the reduced erbium concentration. The deep erbium layer was deposited prior to any GaAs deposition. The erbium present in this layer shows a long tail which must be attributed to diffusion during subsequent growth. Similarly, although RBS indicates that the upper erbium layer was deposited into a very thin high-concentration film, SIMS shows diffusion into the bulk in a very short period of time. The maximum erbium concentration achieved in any sample over the matrix in Table 2 was approximately one atomic percent, as shown in Figure 7, sample number 1876 from Table 2.

Additional measurement techniques were used to quantify the crystal structure of the Er-doped layer. An X-ray rocking curve for sample "1876" with the highest erbium concentration is shown in Figure 8. There is some broadening of the sharp peak compared to "perfect" GaAs due to a small lattice-constant shift for the highly doped layer, and interstitial dopant. A high resolution TEM picture of sample 1878 is shown in Figure 9. After searching carefully, the microscopist could find just one defect (indicated by arrow) at the interface between the substrate and the start of growth. The surface is terraced by growth at 1° off true <100>. The material has good crystal structure.

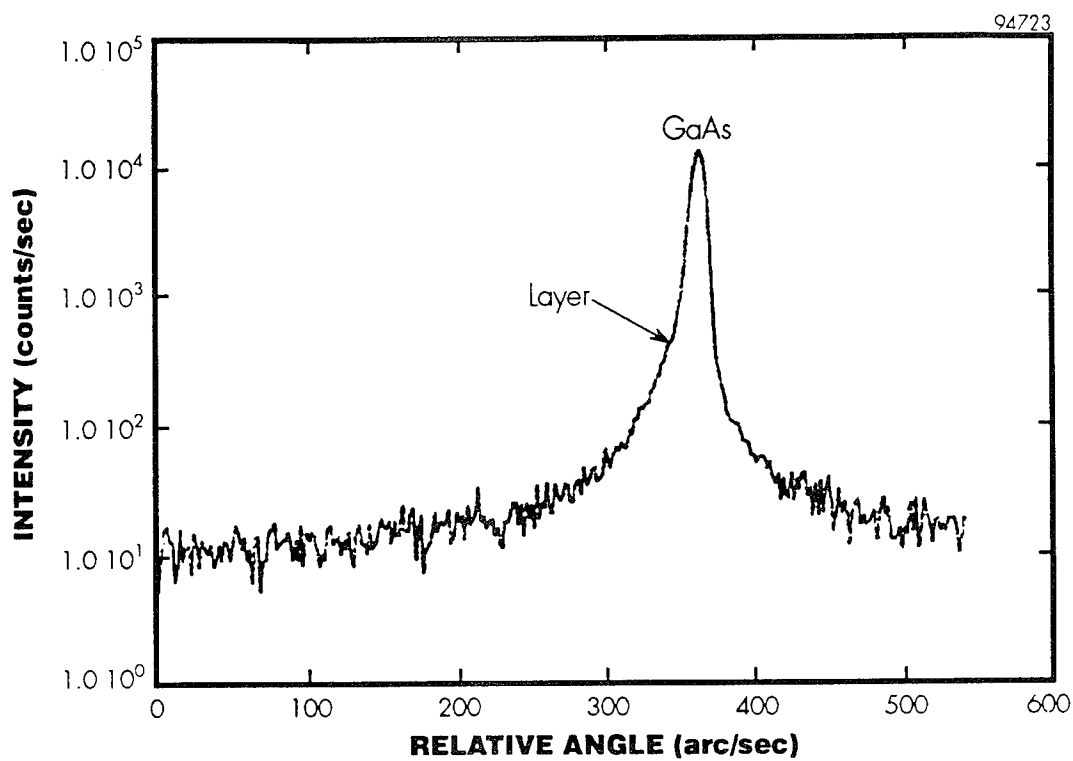


**Figure 8** X-ray rocking curve for  $<200>$  reflection from sample 1878 showing good crystal quality.

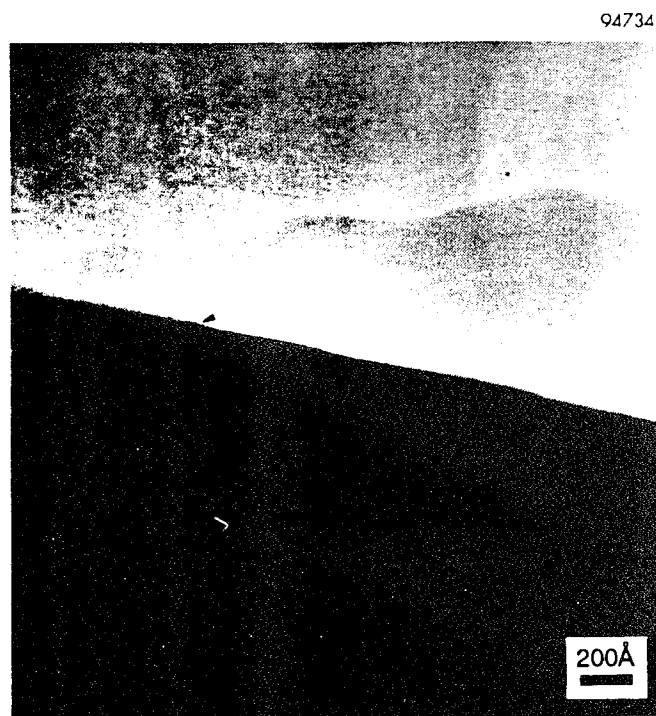


**Figure 9** High magnification TEM microphotograph of erbium doped GaAs layer showing one defect at start of growth (arrow), and terraced surface from substrate alignment  $1^\circ$  off true  $<100>$ .

## 5 CONCLUSIONS AND RECOMMENDATIONS

The objective of this work was to grow an epitaxial film of erbium-arsenide on GaAs by MOCVD, and then deposit an epitaxial film of GaAs on top of the ErAs, also by MOCVD. Spire succeeded in depositing very highly doped erbium layers of GaAs epitaxially with good crystal structure. The pure ErAs phase was not achieved as the diffusion coefficient of interstitial erbium atoms on gallium-arsenide was very high at the deposition temperatures used in this study. Erbium was diffusing into the substrate almost as fast as it was being deposited upon the surface of the sample, preventing accumulation of the true compound ErAs. A rough estimate of the diffusion coefficient for interstitial erbium in GaAs at 650 °C is  $1.3 \times 10^{-15} \text{ cm}^2/\text{sec}$ . An improved determination of the diffusion constant could be done with the available data by modeling the thermal processes during film growth to duplicate the data in Figures 6 and 7.

Epitaxial growth of ErAs on GaAs by MOCVD would be possible with a source that has a high vapor pressure so that the growth rate greatly exceeds the diffusion rate. Alternate Er sources with expected higher vapor pressures have been identified and included in the Phase II proposal.

## 6 REFERENCES

1. J.N. Schulman and T.C. McGill, Appl. Phys. Lett. 34, 663 (1979).
2. R. Fathauer, Technical Support Package for NASA TECH BRIEF, v15, No. 5, item 132, JPL Invention Report NPO-17713/7213 (1990).
3. A. Greenwald, "Ion Doped Quantum Well Lasers", Air Force Contract F49620-92-C-0060, Materials Research Society Symposium Proceedings 301, **21** (1994).
4. C.J. Palmstro *et al.*, Appl. Phys. Lett. 53, 2608 (1988).
5. J.G. Zhu *et al.*, Mat. Res. Soc. Symp. Proc. 160, 325 (1990).
6. C.J. Palstrom *et al.*, J. Vac. Sci. Tech. b7, 747 (1989).
7. P.F. Miceli, *et al.*, Appl. Phys. Lett. 58, 1602 (1991).
8. P.F. Miceli, *et al.*, Mat. Res. Soc. Sym. Proc. 202, 579 (1991).
9. T.G. Finstad *et al.*, ibid. p.413.
10. J.D. Ralston *et al.*, J. Appl. Phys. 68, 2176 (1990).
11. A. Guivarch *et al.*, Mat. res. Soc. Proc. 160, 331 (1990).
12. K. Uwai *et al.*, Appl. Phys. Lett. 51, 1010 (1987).
13. H. Nakagome *et al.*, Appl. Phys. Lett. 53, 1726 (1988).
14. B.J. Heijmink *et al.*, Appl. Phys. Lett. 59, 3279 (1991).
15. S. James Allen *et. al.*, Mat. Res. Soc. Symp. Proc. 301, **307** (1994).

## **LIST OF SYMBOLS, ABBREVIATIONS, and ACRONYMS**

Cp	cyclopentadienyl = C <sub>5</sub> H <sub>5</sub> organic radical
MeCp	methylcyclopentadienyl = C <sub>4</sub> H <sub>3</sub> CH <sub>3</sub>
MOCVD	metalorganic chemical vapor deposition
RBS	Rutherford backscattering spectroscopy
SIMS	secondary ion mass spectroscopy
TBA	tertiarybutyl arsine
TEM	transmission electron microscope